ELSEVIER

www.elsevier.nl/locate/jorganchem

Journal of Organometallic Chemistry 610 (2000) 102–111

Journal of Organometallic Chemistry

# The mutual influence of the imine substituents of terephthal-bis-imines concerning their reactivity towards $Fe_2(CO)_9$ ☆

Wolfgang Imhof *, Angela Göbel

*Institut für Anorganische und Analytische Chemie der Universität, August-Bebel-Straße 2, D-07743 Jena, Germany*

Received 17 April 2000; received in revised form 12 July 2000

**Abstract**

The reaction of terephthal-bis-imines with $Fe_2(CO)_9$ proceeds via a C–H activation reaction in the *ortho* position with respect to one of the imine functions. The corresponding hydrogen atom is shifted towards the former imine carbon atom producing a methylene group instead. The dinuclear iron complexes formed by this reaction sequence and showing no coordination of the second imine group were isolated from reactions of bis-imines with both phenyl and cyclohexyl substituents at the imine nitrogen atoms. In addition, we observed three different reaction pathways of the second imine substituent of the starting material which is obviously thus influenced by the fact that the first one is coordinating an $Fe_2(CO)_6$ moiety. If the organic substituent at the imine nitrogen atoms is a phenyl group the formation of a trinuclear complex is achieved in which an additional $Fe(CO)_3$ group is coordinating the CN double bond and one of the carbon–carbon bonds of the central phenyl ring in an $\eta^4$-fashion. The same reaction leads to the isolation of a tetranuclear iron–carbonyl compound in which both imine substituents were transformed via the pathway described above, each building up dinuclear subunits. In contrast to this the reaction of a bis-imine with cyclohexyl groups at the imine nitrogen and thus an enhanced nucleophilicity leads to the formation of a tetranuclear complex in which only one imine group reacts under C–H activation with subsequent hydrogen migration towards the former imine carbon atom. The second imine substituent also shows a C–H activation reaction in the *ortho* position with respect to the imine group but the corresponding hydrogen atom is transferred to one of the aromatic carbon atom of the central phenyl ring of the ligand. The C=N double bond remains unreacted and only coordinates the second $Fe_2(CO)_6$ moiety via the nitrogen lone pair. 

*Keywords:* C–H activation; Hydrogen migration; Iron; Carbonyl; X-ray structure

## 1. Introduction

C–H activation reactions induced by transition metal compounds are key steps in a lot of catalytic transformations leading to the formation of new C–C bonds and have thus been studied thoroughly during the last number of years [1]. If aromatic compounds bearing functional groups with the potential to act as coordination sites for transition metals are used, the C–H activation step normally takes place regioselectively in terms of an orthometallation reaction [2].

During the last number of years we reported the reaction of $Fe_2(CO)_9$ with imines derived from aromatic aldehydes like benzaldehyde, thiophene-carbaldehyde, pyrrole-carbaldehyde and others. We found that the reactions proceeded via the activation of a C–H bond in the *ortho* position with respect to the exocyclic imine moiety, followed by a 1,3-hydrogen transfer reaction towards the former imine carbon atom, thus forming a methylene group instead [3]. The reaction of imines derived from naphthylcarbaldehydes shows that hydrogen migration may also follow other pathways depending on the substitution position (α- or β-naphthyl derivatives) and the organic subsituent at the imine nitrogen atom [4].

Since aromatic imines may be catalytically reacted with CO and/or olefins in the presence of $Ru_3(CO)_{12}$ to form new C–C bonds regioselectively in the *ortho* posi-

☆ Part of this work has been presented at the XVIIIth Conference on Organometallic Chemistry, 16–21/8/1998, Munich, Germany.

* Corresponding author. Tel.: +49-3641-948128; fax: +49-3641-948102.

*E-mail address:* cwi@rz.uni-jena.de (W. Imhof).

0022-328X/00/$ - see front matter 
PII: S0022-328X(00)00515-5

tion with respect to the imine substituent the reactions of the same organic substrates with $Fe_2(CO)_9$ may well serve as model reactions for the initial steps of catalytic C–C bond formation [5].

In the reaction of imines derived from naphthylcarbaldehydes we saw that hydrogen migration following the C–H activation step is obviously determined by the electronic properties of the starting compound [4]. So, we were interested in the reactions of bifunctional imines with $Fe_2(CO)_9$ in order to see whether the reaction of the iron–carbonyl with one of the imine functions has any significant influence on the reactivity of the second imine moiety. In this report we describe the products that may be obtained from the reaction of bis-imines derived from terephthalaldehyde and $Fe_2(CO)_9$.

## 2. Results and discussion

### 2.1. Synthesis and spectroscopic properties of the compounds

The bis-imines of terephthalaldehyde **1a** and **1b** are easily prepared by the reaction of the aldehyde with two equivalents of the corresponding amine followed by a recrystallization from ethanol [6]. Treatment of **1a** and **1b** with $Fe_2(CO)_9$ in *n*-heptane at 50°C leads to the formation of the organoiron complexes **2**–**5** (Scheme 1).

The dinuclear compounds **2a** and **2b** are the main products of the reaction whereas the product distribution concerning complexes **3**–**5** depends on the organic substituent at the imine nitrogen atom. In **2a** and **2b** one of the imine moieties shows the same reactivity pattern of subsequent C–H activation and 1,3-hydrogen migration as it was previously observed for a series of aromatic imines [3]. The second imine group remains unreacted.

The trinuclear complex **3**, which is only observed in the reaction starting from **1b**, shows the same dinuclear subunit at one of the imine substituents as it is found in **2a** and **2b**. The second imine moiety is involved in the coordination of an $Fe(CO)_3$ group, which may be described in analogy to the well known ($\eta^4$-1-azadiene)$Fe(CO)_3$ complexes [7]. So at the second imine group no C–H activation step takes place.

In addition, there are two different tetranuclear iron–carbonyl complexes formed, of which **4** is only isolated from the reaction of **1a** with $Fe_2(CO)_9$ besides **2a**. On the other hand, the reaction of **1b** yields **5** as well as **2b** and **3**. Both **4** and **5** show that one of the imine substituents builds up the same dinuclear subunit observed for **2a**, **2b** and **3** by a C–H activation reaction in the *ortho* position with respect to the imine group and a subsequent migration of a hydrogen atom towards the former imine carbon atom. In **4** and **5** a second C–H activation is observed, but the two complexes differ in the pathway of hydrogen migration following C–H activation. In **4** the hydrogen atom is transferred towards one of the aromatic carbon atoms of the central phenyl ring of the former terephthalic aldehyde building up a methylene group instead. Only in **5** do both imine subunits of the starting material show the expected reactivity in the reaction with $Fe_2(CO)_9$ building up two dinuclear subunits in which the hydrogen atoms were shifted towards the former imine carbon atoms.

All compounds may easily be identified by their NMR spectroscopic properties. In **2a** and **2b** only one of the imine groups reacted with $Fe_2(CO)_9$. So the $^1$H-NMR spectra show signals characteristic for imine

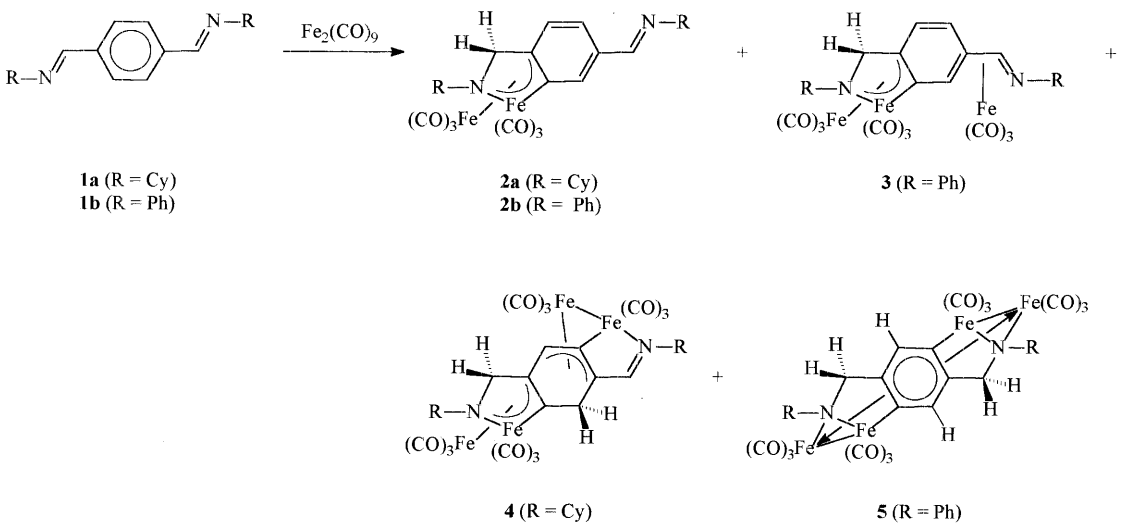


Scheme 1.

hydrogen atoms above 8 ppm as well as resonances representing the methylene groups at the second former imine carbon atom at about 4 ppm. As it was already observed for the reaction of other aromatic imines the signal of the methylene moiety in **2a** and **2b** is observed as a singlet although in principle they are diastereotopic [3,4]. Together with the fact that there is only one carbon resonance for the CO ligands this shows the high fluxionality of the $Fe_2(CO)_6$ moiety in solution. This fluxionality has also been observed for dinuclear ruthenium carbonyl complexes with enyl-amido ligands and has been described as a windshield wiper process [7]. In contrast to the ruthenium complexes the motion of the $Fe(CO)_3$ moieties in **2a** and **2b** may not be frozen since there is no change in the hydrogen NMR spectra when lowering the temperature from 20 to $-85$°C.

In **3** the methylene group, which is formed during the reaction by a C–H activation, 1,3-hydrogen shift reaction sequence, gives rise to a typical AB-spin pattern in the hydrogen NMR. In addition, the $^{13}$C-NMR spectrum shows seven CO resonances with one at 209.9 ppm showing a higher intensity than the other ones. So only one of the $Fe(CO)_3$ groups still shows a free rotation with respect to the ligand whereas the other iron–carbonyl moieties are fixed. The hydrogen atoms of the 1-azadiene subunit which is $\eta^4$-coordinated of the third $Fe(CO)_3$ fragment show signals which are shifted to higher field compared to the free ligand which corresponds very well with results already published in the literature for similar compounds [8].

Complex **4** shows two different methylene groups being formed during the reaction, one at one of the former imine carbon atoms, the second at one of the carbon atoms of the central phenyl ring of the terephthalic aldehyde. Both give rise to AB-spin patterns in the hydrogen NMR between 3.2 and 4.0 ppm. The presence of only two CO resonances in the carbon NMR spectrum of **4** shows the equivalence of the CO ligands within the two different $Fe_2(CO)_6$ moieties. So the observation of both methylene groups as AB systems showing the diastereotopicity of those hydrogen atoms is obviously due to the different coordination modes of the $Fe_2(CO)_6$ fragments adding an additional element of asymmetry to the molecule. The remaining aromatic hydrogen atom of the phenyl ring as well as the second imine double bond show hydrogen resonances at expected values.

Complex **5** also shows two methylene groups, but in contrast to **4** both imine subunits of the free ligand show exactly the same reaction pathway when treated with $Fe_2(CO)_9$. So the molecule exhibits an internal center of symmetry, which is also observed in it's crystal structure (see below), leading to a simplification of the NMR spectra. Both methylene groups are observed as one singlet at 4.21 ppm as are the remaining aromatic hydrogen atoms of the central phenyl moiety at 8.17 ppm. In addition, there is only one CO resonance present in the carbon NMR spectrum again showing the high fluxionality of the organometallic residues.

### *2.1.1. Structure determinations*

By means of recrystallization from mixtures of light petroleum (b.p. 40–60°C) and $CH_2Cl_2$ at $-20$°C it was possible to obtain crystals suitable for X-ray structure determinations for all compounds.

The result of the structure determination of **2a** is shown in Fig. 1, the same atom numbering scheme has been adopted for the structure of **2b**. Selected bond lengths and angles of **2a** and **2b** are summarized in Table 1. In **2a** and **2b** only one of the two imine substituents of the bis-imine has reacted with $Fe_2(CO)_9$. In the *ortho* position with respect to the former C=N double bond (C1=N1) a C–H activation reaction took place and the central phenyl ring is metallated by one of the iron atoms (Fe2). The corresponding hydrogen atom is transferred to the former imine carbon atom producing a methylene group instead. The bond lengths and angles at C1 are typical for a tetrahedrally surrounded $sp^3$ carbon atom. So the ligand may be described as a formally six-electron donating enyl-amido ligand coordinating an $Fe_2(CO)_6$ moiety. The apical

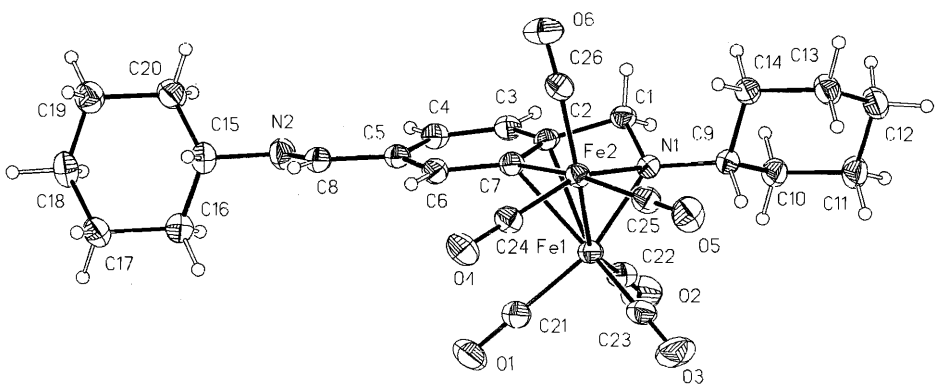


Fig. 1. Molecular structure of **2a**, the numbering scheme has been adopted for the structure analysis of **2b**.

Table 1
Selected bond lengths (pm) and angles (°) of **2a** and **2b**

| | **2a** | **2b** | | **2a** | **2b** |
|---|---|---|---|---|---|
| Fe1–Fe2 | 242.49(5) | 246.1(1) | Fe1–N1 | 197.2(2) | 196.9(3) |
| Fe1–C7 | 221.9(2) | 216.0(4) | Fe1–C2 | 236.6(2) | 229.5(2) |
| Fe2–N1 | 199.0(2) | 198.4(4) | Fe2–C7 | 199.0(2) | 198.2(5) |
| N1–C1 | 147.6(3) | 146.6(7) | C1–C2 | 149.6(3) | 151.5(6) |
| C2–C7 | 142.1(3) | 141.5(7) | C2–C3 | 141.8(3) | 143.0(7) |
| C3–C4 | 135.9(4) | 136.3(6) | C4–C5 | 142.3(4) | 143.2(8) |
| C5–C6 | 136.8(4) | 136.5(8) | C6–C7 | 142.7(4) | 143.5(6) |
| C5–C8 | 147.4(4) | 147.5(6) | C8–N2 | 126.4(3) | 125.7(7) |
| N1–Fe2–C7 | 79.11(9) | 78.4(2) | Fe2–C7–C2 | 130.3(2) | 114.2(3) |
| C7–C2–C1 | 114.8(2) | 113.6(4) | C2–C1–N1 | 102.2(2) | 100.9(4) |
| C1–N1–Fe2 | 112.5(1) | 111.8(3) | C1–C2–C3 | 122.8(2) | 123.9(4) |
| C2–C7–C6 | 115.8(2) | 116.2(4) | C5–C8–N2 | 121.4(2) | 122.6(5) |
| C8–N2–C15 | 118.4(2) | 118.4(5) | | | |

iron atom (Fe1) shows a metal–metal bond and in addition interacts with the former imine nitrogen atom (N1) and one of the aromatic carbon–carbon bonds of the central phenyl ring (C2–C7). The latter interaction shows two significantly different iron–carbon bond lengths. The iron–carbon bond of Fe1 with the carbon atom that is metallated by Fe2 (C7) is about 15 pm shorter than the other iron–carbon bond (Fe1–C2). The same effect has been observed for derivatives of **2a** and **2b** derived from benzaldimines or heterocyclic imines [3]. Another interesting fact is that C5, where the second imine group is situated, shows two aromatic carbon–carbon bonds of different length. The bond towards C6 is about 5 pm shorter than the bond towards C4. So the latter may be more electron deficient compared to C5–C6. The second imine substituent in **2a** and **2b** remains unreacted and thus shows bond lengths and angles of expected values at the corresponding carbon–nitrogen double bond (N2=C8). In both **2a** and **2b** the two carbon–nitrogen bonds adopt a *cis*-arrangement.

The molecular structure of **3** is shown in Fig. 2, the most significant bond lengths and angles are depicted in Table 2. One of the imine groups has reacted as described for **2a** and **2b** building up a dinuclear subunit by C–H activation with subsequent hydrogen migration towards the former imine carbon atom (C1). The bond lengths and angles show the same properties as in **2a** and **2b**. In contrast to **2a** and **2b** the second imine substituent also interacts with an iron–carbonyl fragment. In this case no C–H activation reaction occurs and the $Fe(CO)_3$ moiety coordinates the imine double bond as well as the aromatic carbon–carbon bond (C4–C5) of the central phenyl ring that is neighboring the metallated carbon atom C3. Interestingly it was just this aromatic carbon–carbon bond that we found to be more electron rich compared to the corresponding bond of C5 towards the other the *ortho* position in the structure analysis of **2a**. The iron atom shows an $\eta^4$-coordination to an 1-azadiene type ligand in which the carbon–carbon double bond is part of an aromatic system. Very recently we were able to isolate the first

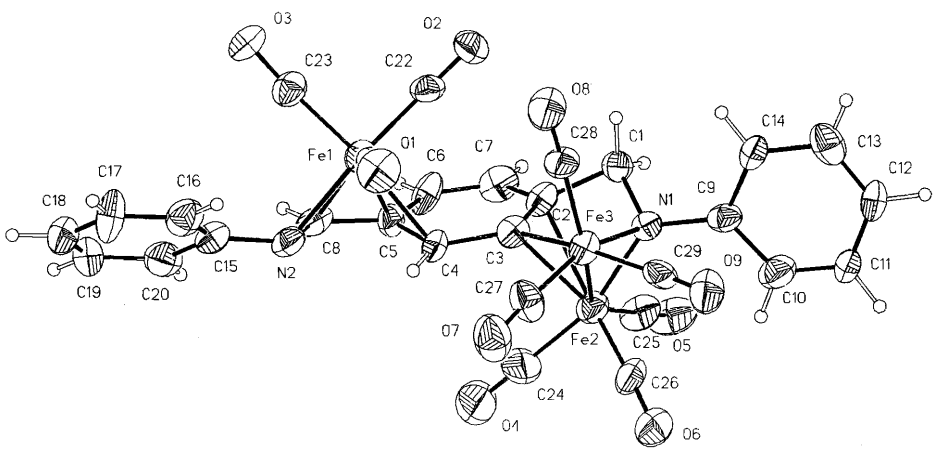


Fig. 2. Molecular structure of **3**.

Table 2
Selected bond lengths (pm) and angles (°) of **3**

| | | | | | |
|---|---|---|---|---|---|
| Fe2–Fe3 | 245.9(3) | Fe2–N1 | 194(1) | Fe2–C2 | 222(1) |
| Fe2–C3 | 214(1) | Fe3–N1 | 197(1) | Fe3–C3 | 201(1) |
| N1–C1 | 150(2) | C1–C2 | 152(2) | C2–C3 | 135(2) |
| C3–C4 | 145(2) | C4–C5 | 145(2) | C5–C6 | 145(2) |
| C6–C7 | 135(2) | C7–C2 | 145(2) | Fe1–C4 | 219(1) |
| Fe1–C5 | 208(1) | Fe1–C8 | 208(1) | Fe1–N2 | 208(1) |
| C5–C8 | 140(2) | C8–N2 | 138(2) | | |
| N1–Fe3–C3 | 77.7(5) | Fe3–C3–C2 | 114(1) | C3–C2–C1 | 117(1) |
| C2–C1–N1 | 97(1) | C1–N1–Fe3 | 113.1(7) | C1–C2–C7 | 119(1) |
| C2–C3–C4 | 120(1) | C3–C4–C5 | 118(1) | C4–C5–C6 | 119(1) |
| C5–C6–C7 | 121(1) | C6–C7–C2 | 119(1) | C7–C2–C3 | 123(1) |
| C4–C5–C8 | 119(1) | C6–C5–C8 | 122(1) | C5–C8–N2 | 116(1) |
| C4–Fe1–C5 | 39.6(5) | C4–Fe1–C8 | 70.3(5) | C4–Fe1–N2 | 79.0(5) |
| C5–Fe1–C8 | 39.5(5) | C5–Fe1–N2 | 69.4(5) | C8–Fe1–N2 | 38.8(5) |

structurally characterized compound of this type from the reaction of an imine derived from β-naphthylcarbaldehyde with $Fe_2(CO)_9$ [4]. On the other hand, this coordination mode has often been reported for iron–carbonyl complexes of acyclic α,β-unsaturated imines [8]. In **3** the coordination of Fe1 to the azadiene subunit of the bis-imine ligand (C4–C5–C8–N2) shows bond lengths and angles typical for ($\eta^4$-1-azadiene)$Fe(CO)_3$ complexes [8]. The most significant feature is the fact that the iron–carbon bond length towards the C-terminal end of the azadiene moiety (C4) is about 10 pm longer than the bond length of Fe1 towards the two central carbon atoms (C5, C8). In our earlier work we were able to show by means of extended Hückel calculations that this observation is due to the fact that there are partial negative charges at C4 and N2, so that the ligand may also be described as a dianionic ligand with a central carbon–carbon double bond coordinating an $Fe^{2+}$ ion [8e].

Fig. 3 shows the molecular structure of **4**, selected bond lengths and angles are summarized in Table 3. **4** is a tetranuclear iron–carbonyl complex in which both imine groups of the starting material interact with $Fe_2(CO)_9$ via a reaction sequence of C–H activation and hydrogen migration. One of the imine substituents shows a dinuclear subunit which is analogous to the one described for **2a** and **2b**. So the C–H activation step also took place in the *ortho* position with respect to the exocyclic imine moiety. The corresponding hydrogen atom was then transferred towards the former imine carbon atom (C8) producing a methylene group instead. In the description of the molecular structures of **2a** and **2b** it was pointed out that the coordination of the apical iron atom (Fe3 in **4**) is unsymmetrical. The same effect is observed in the molecular structure of **4**, but the difference between the bond length of Fe3–C5 and Fe3–C6 is only about 5 pm compared to 15 pm for **2a** and **2b**. The second imine moiety in **4** also reacted via a C–H activation reaction in the *ortho* position with respect to the imine group. The hydrogen atom was then transferred towards one of the aromatic carbon atoms of the central phenyl ring (C7) whereas the imine

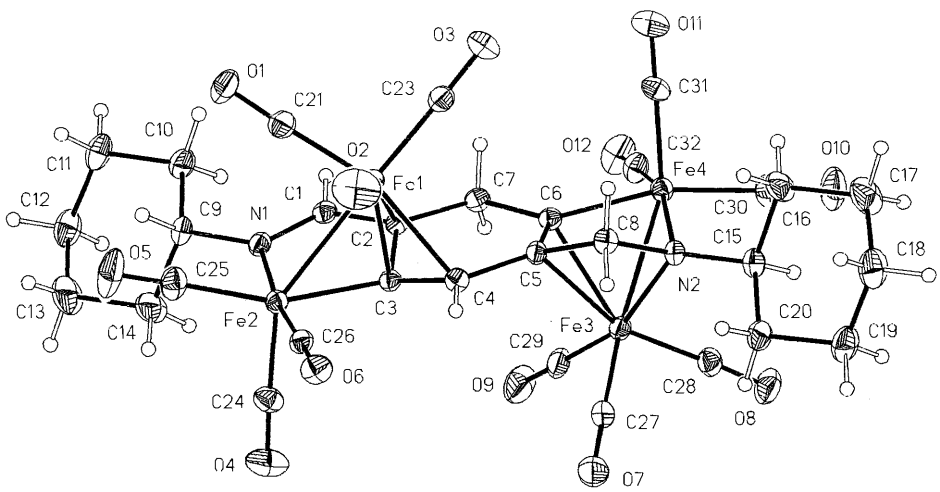


Fig. 3. Molecular structure of **4**.

Table 3
Selected bond lengths (pm) and angles (°) of **4**

| | | | | | |
|---|---|---|---|---|---|
| Fe1–Fe2 | 264.52(7) | Fe1–C2 | 221.3(2) | Fe1–C3 | 196.0(3) |
| Fe1–C4 | 215.9(4) | Fe2–N1 | 201.3(3) | Fe2–C3 | 195.2(3) |
| C1–N1 | 129.0(4) | C1–C2 | 144.8(5) | C2–C3 | 142.4(5) |
| C3–C4 | 142.6(5) | C4–C5 | 147.1(5) | C5–C6 | 140.3(5) |
| C6–C7 | 151.5(5) | C7–C2 | 152.0(5) | Fe3–Fe4 | 245.10(7) |
| Fe3–N2 | 197.4(3) | Fe3–C5 | 220.5(3) | Fe3–C6 | 215.0(3) |
| Fe4–N2 | 197.5(3) | Fe4–C6 | 195.1(3) | N2–C8 | 148.0(4) |
| C8–C5 | 151.1(5) | | | | |
| C2–Fe1–Fe2 | 69.25(8) | C2–Fe1–C3 | 39.3(1) | C2–Fe1–C4 | 65.9(1) |
| C3–Fe1–Fe2 | 47.34(9) | C3–Fe1–C4 | 40.2(1) | C4–Fe1–Fe2 | 78.38(9) |
| Fe1–C3–Fe2 | 85.1(1) | C3–Fe2–N1 | 83.2(1) | Fe2–N1–C1 | 112.9(2) |
| N1–C1–C2 | 116.7(3) | C1–C2–C3 | 114.5(3) | C2–C3–Fe2 | 110.1(2) |
| C2–C3–C4 | 113.2(3) | C3–C4–C5 | 120.6(3) | C4–C5–C6 | 123.1(3) |
| C5–C6–C7 | 117.6(3) | C6–C7–C2 | 114.5(3) | C7–C2–C3 | 123.1(3) |
| Fe4–N2–C8 | 111.9(2) | N2–C8–C5 | 100.1(3) | C8–C5–C6 | 113.4(3) |
| C5–C6–Fe4 | 114.9(2) | C6–Fe4–N2 | 79.2(1) | Fe4–Fe3–N2 | 51.65(8) |
| Fe4–Fe3–C5 | 75.04(9) | Fe4–Fe3–C6 | 49.65(9) | N2–Fe3–C5 | 66.3(1) |
| N2–Fe3–C6 | 74.6(1) | C5–Fe3–C6 | 37.6(1) | | |

double bond remains unreacted and thus shows a bond length of 129 pm. So one of the iron atoms (Fe2) of this $Fe_2(CO)_6$ moiety metallated the phenyl ring (C3) and is coordinated by the lone pair of the imine nitrogen (N1). The apical iron atom (Fe1) beside a metal–metal interaction shows a π-allyl type coordination to three carbon atoms of the former aromatic system (C2, C3, C4). The same hydrogen migration pathway was observed in the reaction of an imine of β-naphthylcarbaldehyde when the organic substituent at the imine nitrogen atom was – as it is in **4** – a cyclohexyl group.

The molecular structure of **5** is shown in Fig. 4, the most important bond lengths and angles are depicted in Table 4. In **5** both imine moieties of the starting material have reacted in exactly the same way. The C–H bonds in the *ortho* position to the imine substituents are activated and the corresponding hydrogen atoms are shifted towards the former imine carbon atom. The middle of the central phenyl ring of the ligand is a crystallographic center of inversion, so the bond lengths and angles in both dinuclear subunits of **5** are identical. The main features of the coordination mode of the $Fe_2(CO)_6$ groups are the same as they were described for **2a** and **2b**. The difference in the bond lengths of the apical iron atom (Fe1) towards the two carbon atoms of the central phenyl ring of the ligand (C2, C3) is about 23 pm and thus this interaction is even more unsymmetrical as it is in **2a** and **2b**.

## 3. Conclusions

This paper describes the synthesis of a number of iron–carbonyl complexes from $Fe_2(CO)_9$ and bis-imines

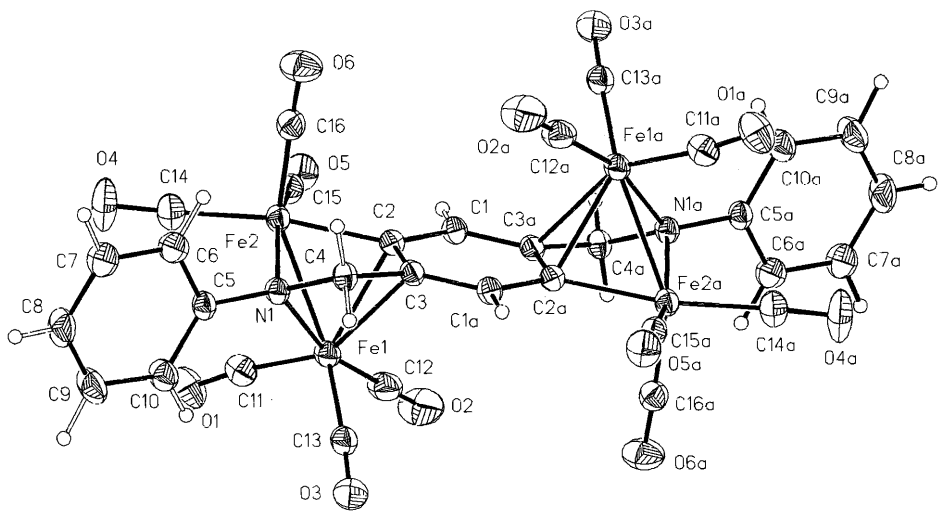


Fig. 4. Molecular structure of **5**.

Table 4
Selected bond lengths (pm) and angles (°) of **5**

| | | | | | |
|---|---|---|---|---|---|
| Fe1–Fe2 | 244.00(6) | Fe1–N1 | 197.1(2) | Fe1–C2 | 218.5(2) |
| Fe1–C3 | 241.4(2) | Fe2–N1 | 197.8(2) | Fe2–C2 | 199.1(2) |
| C2–C3 | 143.2(4) | C3–C4 | 149.6(4) | C4–N1 | 148.0(3) |
| C1–C2 | 140.3(4) | C1–C3a | 139.5(4) | | |
| N1–Fe1–Fe2 | 51.95(6) | C2–Fe1–Fe2 | 50.62(7) | C3–Fe1–Fe2 | 72.55(6) |
| N1–Fe1–C2 | 74.26(9) | N1–Fe1–C3 | 62.71(8) | C2–Fe1–C3 | 35.83(9) |
| N1–Fe2–C2 | 78.63(9) | Fe2–C2–C3 | 113.1(2) | C2–C3–C4 | 114.6(2) |
| C3–C4–N1 | 102.0(2) | C4–N1–Fe2 | 111.8(2) | C1–C2–C3 | 116.5(2) |
| C2–C1–C3a | 121.3(2) | C2–C3–C1a | 122.2(2) | | |

of terephthalaldehyde. In analogy to imines from benzaldehyde and some heterocyclic aldehydes the main reaction is the formation of dinuclear compounds in which a C–H activation reaction occurs in the *ortho* position with respect to the exocyclic imine function. The corresponding hydrogen atom is then transferred towards the former imine carbon atom producing a methylene group instead. This reaction sequence leads to the formation of **2a** and **2b** in which the second imine group of the starting material remains unreacted.

Complexes **3** and **5** are only observed if there is an aromatic substituent present at the imine nitrogen atoms of the ligand. In the formation of **3** the second imine moiety reacts like a 1-azadiene type ligand coordinating a $Fe(CO)_3$ group in an $\eta^4$-fashion with one of the aromatic carbon–carbon bonds interacting with the iron atom. So the reaction of $Fe_2(CO)_9$ with the second imine group does not lead to a C–H activation reaction. The tetranuclear compound **5** shows the reaction sequence described for **2a** and **2b** at both imine substituents of the starting material.

Another tetranuclear compound is isolated if the organic substituent at the imine nitrogen atoms is a cyclohexyl group. In **4** both imine moieties react under C–H activation in the *ortho* position with respect to the imine substituents. The difference in the coordination modes is realized by different migration pathways of the corresponding hydrogen atoms. In one case it is again transferred towards the former imine carbon atom whereas the second hydrogen atom is shifted towards one of the carbon atoms of the former central phenyl ring of the ligand producing another methylene group there.

So in conclusion it may be said that the reaction of the first imine substituent induces three different possibilities concerning the reactivity of the second imine group. Obviously the pathway of the reaction is also controlled by the nature of the organic substituent at the imine nitrogen atom which also determines the basicity of the imine nitrogen atom.

## 4. Experimental

### 4.1. General

All procedures were carried out under an argon atmosphere in anhydrous, freshly distilled solvents. Chromatography was carried out using silica gel 60 and silanized silica gel 60, 70–230 mesh ASTM (Merck), which were dried at $10^{-2}$ bar ($10^3$ Pa) for 2 days before use. Infrared spectra were recorded on a Perkin–Elmer FTIR System 2000 using 0.2-mm KBr cuvettes. NMR spectra were recorded on a Bruker AC 200 spectrometer ($^1$H: 200 MHz, $^{13}$C: 50.32 MHz with $CDCl_3$ as internal standard) or with a Bruker DRX 400 spectrometer ($^1$H: 400 MHz, $^{13}$C: 100.62 MHz with $CDCl_3$ as internal standard). Mass spectra were recorded on a Finnigan MAT SSQ 710 instrument. High-resolution mass spectrometry (HRMS) was carried out using a Finnigan MAT 95 XL instrument with FAB techniques. Elemental analyses were carried out at the laboratory of the Institute of Organic Chemistry and Macromolecular Chemistry of the Friedrich-Schiller-University Jena.

### 4.2. X-ray crystallographic study

Structure determinations were carried out using an Enraf–Nonius Kappa CCD diffractometer, with a crystal detector distance of 25 mm and 180 frames using graphite monochromated Mo–$K_\alpha$ radiation. The crystals were mounted in a stream of cold nitrogen. Data were corrected for Lorentz and polarization effects but not for absorption. The structures were solved by direct methods and refined by full-matrix least-squares techniques against $F^2$ using the programs SHELXS-86 and SHELXL-93 [9]. Computations of the structures were carried out with the program XPMA [10] and the molecular illustrations were drawn using the program XP [11]. The crystal and intensity data are given in Table 5.

Table 5
Crystal and intensity data for the compounds **2a**, **2b**, **3**, **4** and **5**

| | **2a** | **2b** | **3** | **4** | **5** |
|---|---|---|---|---|---|
| Formula | $C_{26}H_{28}Fe_2N_2O_6$ | $C_{26}H_{16}Fe_2N_2O_6$ | $C_{29}H_{16}Fe_3N_2O_9 \cdot 0.5H_2O$ | $C_{32}H_{28}Fe_4N_2O_{12}$ | $C_{32}H_{16}Fe_4N_2O_{12}$ |
| Molecular weight (g mol$^{-1}$) | 576.20 | 564.11 | 713.99 | 855.96 | 843.87 |
| Radiation | Mo–$K_\alpha$ | Mo–$K_\alpha$ | Mo–$K_\alpha$ | Mo–$K_\alpha$ | Mo–$K_\alpha$ |
| Monochromator | Graphite | Graphite | Graphite | Graphite | Graphite |
| Temperature (K) | 183 | 183 | 183 | 203 | 183 |
| Crystal color | Red | Red | Red | Brown | Brown |
| Crystal size | $0.9 \times 0.2 \times 0.02$ | $0.4 \times 0.2 \times 0.02$ | $0.8 \times 0.05 \times 0.01$ | $0.2 \times 0.15 \times 0.01$ | $0.2 \times 0.2 \times 0.2$ |
| $a$ (Å) | 13.7200(5) | 8.973(1) | 9.894(4) | 15.9797(5) | 9.353(1) |
| $b$ (Å) | 14.3621(3) | 23.963(2) | 11.876(5) | 9.0006(4) | 12.817(2) |
| $c$ (Å) | 13.2129(5) | 11.664(2) | 14.303(6) | 25.522(1) | 14.101(2) |
| $\alpha$ (°) | 90 | 90 | 109.05(3) | 90 | 90 |
| $\beta$ (°) | 97.42(2) | 103.268(5) | 98.50(2) | 106.149(2) | 104.91(1) |
| $\gamma$ (°) | 90 | 90 | 98.07(3) | 90 | 90 |
| Volume (Å$^3$) | 2581.8(2) | 2441.0(5) | 1539(1) | 3525.9(2) | 1633.6(4) |
| $Z$ | 4 | 4 | 2 | 4 | 2 |
| $F(000)$ | 1192 | 1144 | 716 | 1736 | 844 |
| $D_{calc}$ (g cm$^{-3}$) | 1.482 | 1.535 | 1.537 | 1.612 | 1.716 |
| Crystal system | Monoclinic | Monoclinic | Triclinic | Monoclinic | Monoclinic |
| Space group | $P2_1/c$ | $P2_1/n$ | $P\bar{1}$ | $P2_1/n$ | $P2_1/c$ |
| Absorption coefficient (mm$^{-1}$) | 1.167 | 1.236 | 1.455 | 1.681 | 1.808 |
| $\theta$ Range | $5.46 < \theta < 23.24$ | $3.46 < \theta < 23.29$ | $3.50 < \theta < 23.28$ | $3.41 < \theta < 23.35$ | $3.39 < \theta < 23.34$ |
| Scan mode | $\varphi$-scan, $\omega$-scan | $\varphi$-scan, $\omega$-scan | $\varphi$-scan, $\omega$-scan | $\varphi$-scan, $\omega$-scan | $\varphi$-scan, $\omega$-scan |
| Reflections measured | 6724 | 5390 | 4019 | 9104 | 4311 |
| Independent reflections | 3449 | 3137 | 4019 | 5001 | 2237 |
| $R_{int}$ | 0.0184 | 0.0738 | 0.0000 | 0.0369 | 0.0457 |
| Reflections observed ($F_o^2 > 2\sigma(F_o^2)$) | 3112 | 2002 | 1777 | 3946 | 2067 |
| Number of parameters | 353 | 340 | 401 | 477 | 258 |
| Goodness-of-fit | 1.082 | 0.871 | 0.985 | 0.995 | 1.061 |
| $R_1$ | 0.0312 | 0.0426 | 0.0909 | 0.0342 | 0.0340 |
| $wR_2$ | 0.0790 | 0.0963 | 0.1994 | 0.0776 | 0.0884 |
| Final diffraction map electron density peak and hole (e Å$^{-3}$) | 0.285, −0.411 | 0.222, −0.255 | 0.522, −0.349 | 0.506, −0.399 | 0.364, −0.467 |

### 4.3. Preparation of the compounds

In a typical experiment a 500 mg sample of $Fe_2(CO)_9$ (1.37 mmol) is stirred together with a slight excess of the corresponding imine (1.5 mmol, **1a**: 447 mg, **1b**: 429 mg) in 40 ml *n*-heptane at 55°C. The reaction is stopped after all of the starting material is dissolved. If the starting compound is **1a** the reaction is completed after 40 min and the color of the solution has changed from light-yellow to reddish-brown. The reaction of **1b** takes 1.5 h to complete, after which time the color of the solution is deep-red. After evaporation of all volatile material in vacuo the oily residue is dissolved in 10 ml $CH_2Cl_2$ and 1 g of silanized silica gel is added. The solvent is again evaporated and the product mixture is separated by means of a column chromatography under inert conditions using mixtures of light petroleum (b.p. 40–60°C) and $CH_2Cl_2$ as the eluent. The reaction of **1a** yields 154 mg of **4** (12%, 20:1 light petroleum–$CH_2Cl_2$) and 372 mg of **2a** (43%, 5: 1 light petroleum–$CH_2Cl_2$). The reaction of **1b** produces 116 mg of **5** (9%, 10: 1 light petroleum–$CH_2Cl_2$), 211 mg of **3** (20%, 3:1 light petroleum–$CH_2Cl_2$) and 296 mg of **2b** (35%, 1:2 light petroleum–$CH_2Cl_2$). All compounds may be recrystallized from mixtures of light petroleum and $CH_2Cl_2$ at −20°C to yield crystals suitable for X-ray structure analyses.

### 4.4. Analytical data for **2a**

MS (FAB) $m/z$: 577 ($MH^+$), 549 [$MH^+ - CO$], 521 ($MH^+ - 2CO$), 492 [$M^+ - 3CO$], 465 ($MH^+ - 4CO$), 436 [$M^+ - 5CO$], 408 [$M^+ - 6CO$]. HRMS $C_{26}H_{28}N_2O_6Fe_2$ (576.21): 577.0717, $C_{26}H_{29}N_2O_6Fe_2$ ($MH^+$), $\Delta = 0.733475$ mmu. IR (Nujol, 293 K) (cm$^{-1}$): 2061m, 2030sh, 2016vs, 1981vs, 1971s, 1961m, 1954m, 1643w. $^1$H-NMR ($CDCl_3$, 293 K) (ppm): 1.03–1.83 (m, 20H, $CH_2$), 2.17–2.26 (m, 1H, CH), 3.05–3.23 (m, 1H, CH), 3.89 (s, 2H, $CH_2$), 7.48 (d, 1H, $^3J_{HH} = 8.5$ Hz, CH), 7.86 (d, 1H, $^3J_{HH} = 8.5$ Hz, CH), 8.11 (s, 1H, CH), 8.24 (s, 1H, N=CH). $^{13}$C-NMR ($CDCl_3$, 293 K) (ppm): 24.7 ($CH_2$), 25.7 ($CH_2$), 26.0 ($CH_2$), 26.2 ($CH_2$), 34.4 ($CH_2$), 35.4 ($CH_2$), 64.8 (CH), 69.9 (CH), 74.2 ($CH_2$), 124.6 (C), 128.4 (CH), 128.5 (CH), 134.3 (C),

145.8 (C), 152.1 (CH), 157.8 (N=CH), 209.8 (CO), 210.4 (CO).

### 4.5. Analytical data for **4**

MS (FAB) $m/z$: 856 [$M^+$], 828 [$M^+ - CO$], 800 [$M^+ - 2CO$], 772 [$M^+ - 3CO$], 744 [$M^+ - 4CO$], 716 [$M^+ - 5CO$], 688 [$M^+ - 6CO$], 660 [$M^+ - 7CO$], 632 [$M^+ - 8CO$], 604 [$M^+ - 9CO$], 576 [$M^+ - 10CO$], 548 [$M^+ - 11CO$]. HRMS $C_{32}H_{28}N_2O_{12}Fe_4$ (855.96): 855.90186, $C_{32}H_{28}N_2O_{12}Fe_4$ [$M^+$], $\Delta = -2.10805$ mmu. IR (Nujol, 293 K) ($cm^{-1}$): 2067sh, 2053s, 2026vs, 1990m, 1979vs, 1970sh, 1957sh, 1941m. $^1$H-NMR ($CDCl_3$, 293 K) (ppm): 0.83–2.05 (m, 21H, $CH_2$, CH), 3.20 (m, 1H, CH), 3.27 (d, $^2J_{HH} = 21.5$ Hz, 1H, $CH_2$), 3.53 (d, $^2J_{HH} = 9.1$ Hz, 1H, $CH_2$), 3.55 (d, $^2J_{HH} = 21.5$ Hz, 1H, $CH_2$), 3.96 (d, $^2J_{HH} = 9.1$ Hz, 1H, $CH_2$), 5.41 (s, 1H, CH), 8.04 (s, 1H, N=CH). $^{13}$C-NMR ($CDCl_3$, 293 K) (ppm): 25.3 ($CH_2$), 25.5 ($CH_2$), 25.7 ($CH_2$), 25.9 ($CH_2$), 26.0 ($CH_2$), 26.3 ($CH_2$), 33.9 ($CH_2$), 34.3 ($CH_2$), 34.6 ($CH_2$), 36.6 ($CH_2$), 44.7 ($CH_2$), 66.3 ($CH_2$), 70.0 (CH), 73.6 (CH), 74.6 (CH), 90.1 (C), 100.9 (C), 166.6 (C), 178.6 (CH), 194.6 (C), 207.1 (CO), 210.4 (CO).

### 4.6. Analytical data for **2b**

MS (FAB) $m/z$: 565 ($MH^+$), 537 [$MH^+ - CO$], 508 [$M^+ - 2CO$], 480 [$M^+ - 3CO$], 453 ($MH^+ - 4CO$), 424 [$M^+ - 5CO$], 397 ($MH^+ - 6CO$). HRMS $C_{26}H_{16}N_2O_6Fe_2$ (564.11): 563.9709, $C_{26}H_{16}N_2O_6Fe_2$ [$M^+$], $\Delta = -0.19192$ mmu. IR (Nujol, 293 K) ($cm^{-1}$): 2066m, 2029vs, 1996s, 1986s, 1970s, 1933m, 1590w. $^1$H-NMR ($CDCl_3$, 293 K) (ppm): 4.41 (s, 2H, $CH_2$), 7.07–7.71 (m, 10H, CH), 7.69 (d, 1H, $J_{HH} = 8.2$ Hz, CH), 8.04 (d, 1H, $J_{HH} = 8.2$ Hz, CH), 8.30 (s, 1H, CH), 8.44 (s, 1H, N=CH). $^{13}$C-NMR ($CDCl_3$, 293 K) (ppm): 75.0 ($CH_2$), 120.3 (C), 120.9 (CH), 122.6 (CH), 125.6 (CH), 126.3 (CH), 127.8 (CH), 129.0 (CH), 129.2 (CH), 129.8 (CH), 134.3 (C), 149.5 (C), 151.7 (C), 152.5 (CH), 158.5 (C), 159.1 (N=CH), 209.6 (CO), 210.0 (CO).

### 4.7. Analytical data for **3**

MS (FAB) $m/z$: 705 ($MH^+$), 648 [$M^+ - 2CO$], 620 [$M^+ - 3CO$], 592 [$M^+ - 4CO$], 565 ($MH^+ - 5CO$), 536 [$M^+ - 6CO$], 508 [$M^+ - 7CO$], 480 [$M^+ - 8CO$], 424 [$M^+ - 8CO - Fe$]. HRMS $C_{29}H_{16}N_2O_9Fe_3$ (704.00): 704.89451, $C_{29}H_{17}N_2O_9Fe_3$ ($MH^+$), $\Delta = 3.70292$ mmu. IR (Nujol, 293 K) ($cm^{-1}$): 2070m, 2054m, 2030vs, 1996sh, 1986vs, 1978sh, 1951m, 1592 (C=N). $^1$H-NMR ($CDCl_3$, 293 K) (ppm): 4.02 (d, $^2J_{HH} = 9.8$ Hz, 1H, $CH_2$), 4.17 (d, $^2J_{HH} = 9.8$ Hz, 1H, $CH_2$), 4.42 (s, 1H, CH), 6.92–7.22 (m, 13H, CH). $^{13}$C-NMR ($CDCl_3$, 293 K) (ppm): 75.3 ($CH_2$), 75.4 (CH), 92.9 (C), 95.0 (C), 101.8 (CH), 121.8 (CH), 122.0 (CH), 122.9 (CH), 124.7 (CH), 125.5 (CH), 128.9 (CH), 128.9 (CH), 129.0 (CH), 152.8 (C), 158.0 (C), 172.0 (C), 204.6 (CO), 206.3 (CO), 208.8 (CO), 209.9 (CO), 210.0 (CO), 211.5 (CO), 212.5 (CO).

### 4.8. Analytical data for **5**

MS (FAB) $m/z$: 844 [$M^+$], 816 [$M^+ - CO$], 788 [$M^+ - 2CO$], 760 [$M^+ - 3CO$], 732 [$M^+ - 4CO$], 704 [$M^+ - 5CO$], 676 [$M^+ - 6CO$], 648 [$M^+ - 7CO$], 620 [$M^+ - 8CO$], 592 [$M^+ - 9CO$], 564 [$M^+ - 10CO$]. IR (Nujol, 293 K) ($cm^{-1}$): 2058s, 2022vs, 1999m, 1986s, 1974s, 1966s, 1951m, 1940m. $^1$H-NMR ($CDCl_3$, 293 K) (ppm): 4.42 (s, 4H, $CH_2$), 7.08–7.28 (m, 8H, CH), 8.17 (s, 2H, N=CH). $^{13}$C-NMR ($CDCl_3$, 293 K) (ppm): 73.3 ($CH_2$), 122.5 (CH), 125.5 (CH), 127.3 (C), 129.0 (CH), 148.6 (C), 151.0 (CH), 158.8 (C), 210.0 (CO).

## 5. Supplementary material

Crystallographic data for the structural analysis has been deposited with the Cambridge Crystallographic Data Centre, CCDC nos. 143603 (**2a**), 143604 (**2b**), 143605 (**3**), 143606 (**4**) and 143607 (**5**). Copies of this information may be obtained free of charge from: The Director, CCDC, 12 Union Road, Cambridge, CB2 1EZ, UK (Fax: +44-1223-336033; e-mail: deposit@ccdc.cam.ac.uk or www: http://www.ccdc.cam.ac.uk).

## Acknowledgements

The authors gratefully acknowledge financial support by the Deutsche Forschungsgemeinschaft (SFB 436).

## References

[1] (a) Y. Guari, S. Sabo-Etienne, B. Chaudret, Eur. J. Inorg. Chem. (1999) 1047. (b) G. Dyker, Angew. Chem. 111 (1999), 1808.
[2] (a) M.I. Bruce, Angew. Chem. 89 (1977) 75. (b) M. Brookhart, M.L.H. Green, J. Organomet. Chem. 250 (1983) 395. (c) E.C. Constable, Polyhedron 3 (1984) 1037. (d) A.E. Ryabov, Chem. Rev. 90 (1990) 403. (e) J. Dehand, M. Pfeffer, Pure Appl. Chem. 3 (1992) 335. (f) A.S. Goldman, Nature 366 (1993) 514. (g) S. Murai, F. Kakiuchi, S. Sekine, Y. Tanaka, A. Kamatani, M. Sonoda, N. Chatani, Pure Appl. Chem. 66 (1994) 1527. (h) F. Kakiuchi, S. Sekine, Y. Tanaka, A. Kamatani, M. Sonoda, N. Chatani, S. Murai, Bull. Chem. Soc. Jpn. 66 (1995) 62. (i) B.M. Trost, Angew. Chem. 107 (1995) 285. (k) A. Sen, Acc. Chem. Res. 31 (1998) 550.
[3] (a) W. Imhof, J. Organomet. Chem. 533 (1997) 31. (b), W. Imhof, J. Organomet. Chem. 541 (1997) 109. (c) W. Imhof, A. Göbel, D. Ohlmann, J. Flemming, H. Fritzsche, J. Organomet. Chem. 584 (1999) 33.
[4] W. Imhof, Organometallics 18 (1999) 4845.

[5] (a) F. Kakiuchi, M. Yamauchi, N. Chatani, S. Murai, Chem. Lett. (1996) 111. (b) T. Fukuyama, N. Chatani, F. Kakiuchi, S. Murai, J. Org. Chem. 62 (1997) 5647. (c) D. Berger, W. Imhof, J. Chem. Soc., Chem. Commun. (1999) 1457. (d) D. Berger, W. Imhof, Tetrahedron 56 (2000) 2015.

[6] **1a**: (a) J.G. Smith, I. Ho, J. Org. Chem. 38 (1973) 2776. (b) N.J. Corville, E.W. Neuse, J. Org. Chem. 42 (1977) 3485. **1b**: (c) L. Horner, E. Jürgens, Chem. Ber. 90 (1957) 2184.

[7] (a) W.P. Mul, C.J. Elsevier, L.H. Polm, K. Vrieze, M.C. Zoutberg, D. Heijdenrijk, C.H. Stam, Organometallics 10 (1991) 2247. (b) W. Imhof, J. Chem. Soc., Dalton Trans. (1996) 1429.

[8] (a) A. De Cian, R. Weiss, Acta Crystallogr. Sect. B 28 (1972) 3264. (b) H.-J. Knölker, G. Baum, P. Gonser, Tetrahedron Lett. 36 (1995) 8191. (c) H.-J. Knölker, H. Goesmann, P. Gonser, Tetrahedron Lett. 37 (1996) 6543. (d) L.A.P. Kane-Maguire, S.G. Pyne, A.F.H. Siu, B.W. Skelton, J. Aust. Chem. 49 (1996) 673. (e) W. Imhof, A. Göbel, D. Braga, P. DeLeonardis, E. Tedesco, Organometallics 18 (1999) 736. (f) D. Berger, M. Dubs, A. Göbel, W. Imhof, M. Kötteritzsch, M. Rost, B. Schönecker, Tetrahedron: Asymmetry 10 (1999) 2983.

[9] (a) G. Sheldrick, SHELXS-86, Universität Göttingen, 1986. (b) G. Sheldrick, SHELXL-93, Universität Göttingen, 1993.

[10] L. Zsolnai, G. Huttner, XPMA, Universität Heidelberg, 1996.

[11] Siemens Analytical X-ray Instruments Inc., XP-INTERACTIVE Molecular Graphics, Version 4.2, 1990.